

Supplementary Materials:

Jianping Cao ^{1,2}, Li Zhang ¹, Zhibin Cheng ¹, Siqi Xie ¹, Runze Li ¹, Ying Xu ³ and Haibao Huang ^{1,2,*}

Section S1. Details of solid-phase microextraction (SPME)

Figure S1 shows the typical structure of solid-phase microextraction (SPME). SPME comprises a plunger (including plunger cap, stainless-steel rod attached to the cap, stainless-steel microtube surrounding the rod, and sealing gasket attached to the microtube) and a sampling fiber. The sampling fiber consists of a cylindrical fused silica fiber with a coating surrounding it (**Figure S1b**). Note, the sampling fiber is not shown in **Figure S1c** because it has been retracted into the microtube to avoid damaging.

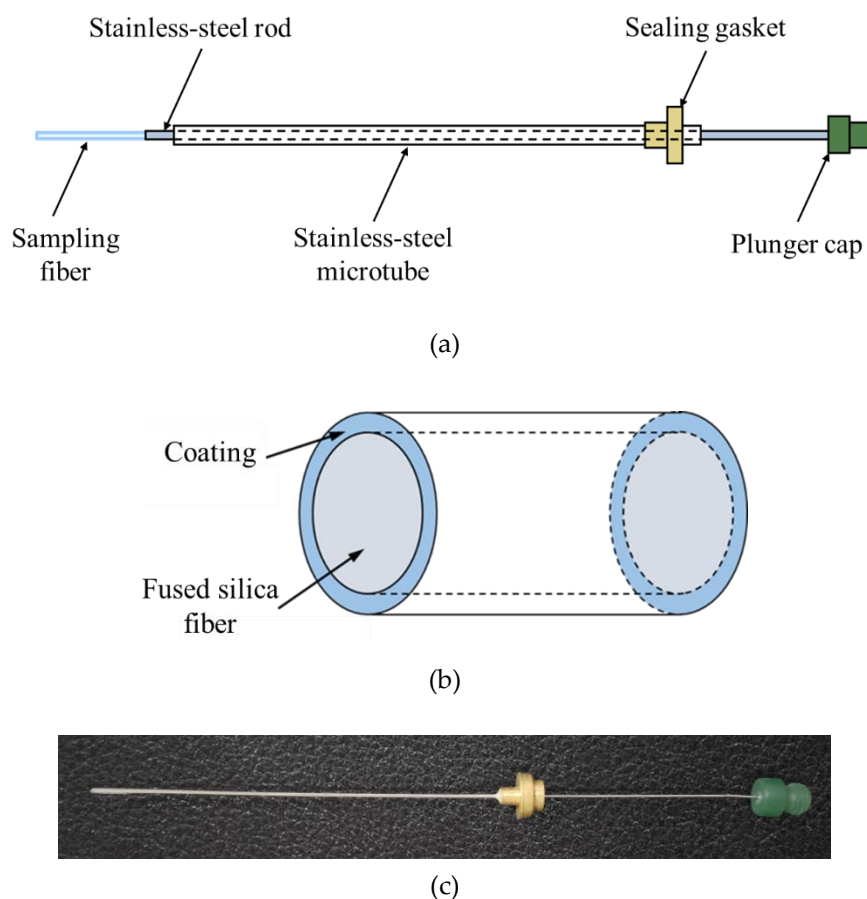


Figure S1. (a) Structure of solid-phase microextraction (SPME), (b) schematic of the sampling fiber, and (c) photo of the SPME used in this study.

The SPME used in this study was purchased from Sigma-Aldrich Co. LLC. (Supelco Analytical, Cat. No. 57302). The SPME coating is made of polydimethylsiloxane (PDMS, feasible for sampling of nonpolar SVOCs [1,2]) with a length of 1 cm and thickness of 7 μm . The fused silica fiber has a length of 1 cm and diameter of 110 μm . The stainless-steel rod has a length of around 10 cm and diameter of around 300 μm . The stainless-steel microtube has a length of around 6 cm and external diameter of around 600 μm . The inner diameter of the microtube is slightly greater than the diameter of the stainless-steel rod.

Figure S2 shows the sorption process of SVOCs by the coating of SPME, i.e., the time variation of the amount of SVOCs sorbed by the SPME coating. As shown, the sorption process can be divided into three regimes: linear, kinetic, and equilibrium. If the time is sufficiently short, the sorption rate of SVOCs by the coating can be treated as a constant, and the sorption amount linearly increases as the time increases. The maximum time of the linear regime (t_1 in Figure S2) is often defined as the time that the sorbed amount reaches 50% of the equilibrium amount [3]. As the time increases, the sorption process becomes the kinetic regime that the sorption rate gradually decreases. In the kinetic regime, the model describing the sorption process is often quite complicated [1]. Finally, the sorption process steps into the equilibrium regime. The minimum time of the equilibrium regime (t_2 in Figure S2) is often defined as the time that the sorbed amount reaches 95% of the equilibrium amount [1].

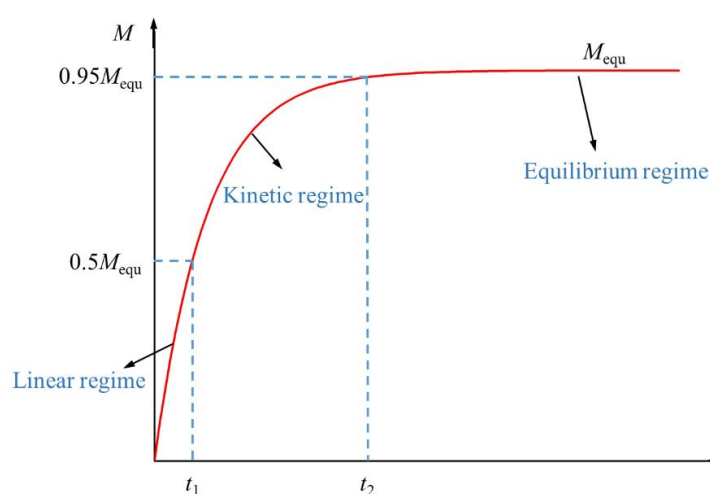


Figure S2. Sorption process of SVOCs by the fiber coating of SPME. M is the amount of SVOCs sorbed by the SPME coating, t is the time of sorption, and M_{equ} is the amount of SVOCs sorbed by the SPME coating when the sorption process reaches equilibrium.

Section S2. Details of the sampling times

1. The sampling time of the sorbent tubes

The sampling time of the sorbent tubes was adjusted according to the concentrations of the target SVOCs to guarantee that the collected SVOC amount was in range of the calibration line of sorbent tubes (100–800 ng, see details below). Because the gaseous SVOC concentration increases as increasing temperature, the sampling time of sorbent tubes should be reduced as increasing temperature. According to our pre-experiments, the sampling times of sorbent tubes for diisobutyl phthalate (DiBP) and tris(1-chloro-2-propyl) phosphate (TCPP) at different temperatures were determined, as listed in Table S1.

Table S1. Sampling times of the sorbent tubes in our experiments (min).

Analytes	Experimental temperatures				
	20 °C	23 °C	25 °C	27 °C	30 °C
DiBP	15	12	10	6	5
TCPP	30	20	15	10	7

2. Determination of the sampling time for SPME

To determine the maximum time of the linear regime in SPME sampling of DiBP and TCPP, a series of pre-experiments were conducted in this study. The experimental system was similar to that introduced in the main text, except that the sampling tube of the SPME-based active sampler was eliminated in the pre-experiments (i.e., Step 2 in “Experiment 1”). In other words, the tee connector of the SPME sampler was directly connected to the outlet of the source chamber. SPMEs were inserted into the outlet of the source chamber (located on the central axis of the source chamber) for different lengths of time, so as to get the time-dependent curve of the SVOC amount sorbed by SPME. The pre-experiments were conducted at 25 °C, with a flow rate of 75 mL/min. The sampling time of SPME ranged from 30 s to 1800 s.

The results of the pre-experiments are shown in Figure S3. Note, we just determined the “equivalent” sorption amount of DiBP and TCPP in the coating of SPME by treating SPME as the liquid samplers.

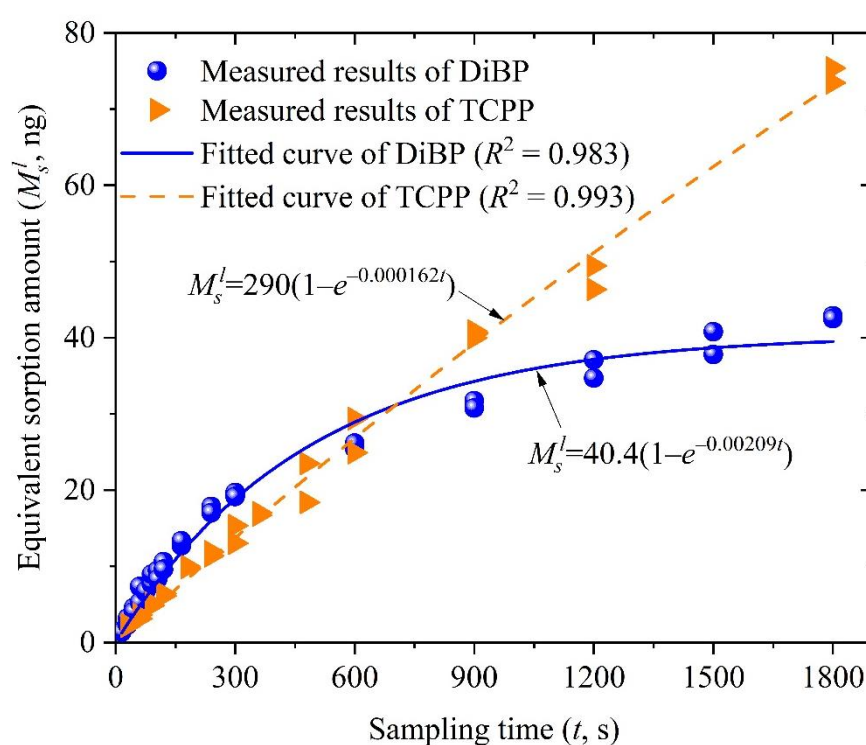


Figure S3. Sorption processes of DiBP and TCPP by the fiber coating of SPME measured in the pre-experiments.

As shown, the sorption process of SPME is close to equilibrium after 1800 s for DiBP, while the sorption process is far from equilibrium for TCPP. In addition, the measured data fits well with an exponential function that has been proposed to describe the sorption process of SPME, $M = M_{equ} \times (1 - \exp(-at))$ [4,5]. The maximum time of the linear sorption (t_1 in Figure S2) was defined as the time that the sorbed amount is less than 50% of the equilibrium amount according to existing study [3], i.e., $t_1 = -(\ln 0.5)/a = 0.693/a$. Substituting the values fitted in Figure S3 into the equation, the maximum times of the linear regime were estimated to be 332 s and 4278 s for DiBP and TCPP, respectively. Therefore, the SPME sampling times of DiBP and TCPP should be shorter than 332 s and 4278 s, respectively. Certainly, the above criteria can just be treated as the approximations of the upper limit of the SPME sampling times. In applications, whether the sampling time is appropriate should be further verified by evaluating the linear relationship between the sampling time and the “equivalent” sorption amount.

In addition, the “equivalent” sorption amount should not exceed the upper limit of the quantitative range of the analytical instrument. In this study, the upper limits of DnBP and TCPP were found to be 30 ng and 40 ng, respectively, because the instrument responses were found to be not linearly related to the “equivalent” sorption amount above these levels (see details below, [Section S3](#)). Therefore, the sampling time should not be too long to ensure that the sampled amount of SVOCs falls in the quantitative range. According to the results in [Figure S3](#), the sampling times of DiBP and TCPP should be shorter than 650 s and 916 s, respectively.

According to the above two limits (linear regime and quantitative limit), the sampling times of DiBP and TCPP should be shorter than 332 s and 916 s, respectively. Therefore, in the experiments of the main text, the longest sampling times of DiBP and TCPP were set to be 300 s and 600 s, respectively. In order to verify the linear relationship between the sampling time and the “equivalent” sorption amount, a series of SPME measurements with different sampling times were conducted in “experiment 1” of the main text. The detailed sampling time series are listed in [Table S2](#). And in “experiment 2” of the main text, only one sampling time was selected for each SVOC, which was approximately in the middle of the time series listed in [Table S2](#), i.e., 120 s for DiBP and 300 s for TCPP.

Table S2. Sampling times of SPME in “experiment 1” of the main text.

Analytes		Sampling times (s)				
DiBP	15	30	60	120	210	300
TCPP	30	60	120	300	450	600

Section S3. Details of chemical analysis

1. GC-MS analysis

All samples were analyzed by a gas chromatography-mass spectrometry system (GC-MS, Agilent Technologies 8890 GC system equipped with a 5977B Mass Selective Detector). The chromatographic column was a fused silica capillary column (HP-5MS, 30 m × 0.25 mm (i.d.) × 0.25 µm film thickness) and the carrier gas was high purity helium (purity > 99.999%). The temperatures of the injector and the ion source were 280 °C and 250 °C, respectively. The GC was operated in the splitless mode. The column temperature program for DiBP was 100 °C, held for 2 min, increased to 300 °C at 10 °C/min, and then held for 5 min (27 min in total); the flow rate of carrier gas was 1.5 mL/min. And for TCPP, the column temperature program was 50 °C, held for 1 min, increased to 240 °C at 4 °C/min, and then held for 1 min (23 min in total); the flow rate of the carrier gas was 1.2 mL/min. The MS was operated in both Scan (mass range 35–400 AMU) and SIM (Selected Ion Monitoring) acquisition modes. The target compounds were quantified using the selected fragment ions, i.e., $m/z = 149$ for DiBP, $m/z = 99$ for TCPP, and $m/z = 105$ for benzyl benzoate (BB, internal standards).

The injection modes of GC-MS were quite different for SPME samples, sorbent tubes, and liquid standards (the liquid standards were used for obtaining k_i in eqs. (1) and (3) of the main text), as noted below:

1) For SPME samples, the SPME was manually insert to the front injector of GC (liner of GC injector: 5190-4048, Agilent Tech.), and thermally desorbed in the injector for 5 min (280 °C). The sampled SVOCs can be desorbed from the SPME coating and be directly transferred to the GC column. According to our measurements, the sampled SVOCs can be completely desorbed after the five-minute desorption at 280 °C.

2) For sorbent tubes, the analysis was conducted by a thermal desorber (UNITY-xr, Markes International) connected to the back injector of the above GC-MS. Before analysis, 2 µL solution of BB (100 µg/mL, 200 ng in total) in dichloromethane (DCM) was injected into the sorbent tubes as internal standards. The sorbent tubes were then desorbed for 30 min at 350 °C (desorption efficiency of the collected SVOCs has been verified to be greater

than 95% through pre-experiments), with a nitrogen flow of 50 mL/min, and a cold trap temperature of 5 °C. After desorption, flash heating the cold trap to 350 °C (held for 5 min) to transfer the analytes to the GC column through the transfer line at 250 °C. While heating, the cold trap was operated at a splitting mode. For DiBP, the cold trap was purged with helium at a flow rate of 31.5 mL/min: 1.5 mL/min of the flow were directed to the GC column, the other 30 mL/min were not used and instead vented through the exhaust. For TCPP, the cold trap was purged with helium at a flow rate of 51.2 mL/min: 1.2 mL/min of the flow were directed to the GC column, the other 50 mL/min were vented through the exhaust.

3) For liquid standards, 1 µL of the standard solution was injected into the front injector of GC (liner of GC injector: 5190-3163, Agilent Tech).

Note: there are two injectors in the GC used in this study, front injector and back injector. The thermal desorber was connected to the back injector (for the treatment of sorbent tubes). And the front injector was used for SPME samples and liquid standards (as noted above, the liners were different for SPME samples and liquid standards).

2. The calibration of GC-MS by injecting liquid standards

Standard solutions of DiBP with six different concentrations (0.6, 1.5, 3, 6, 24 and 30 µg/mL) were obtained by diluting DiBP liquids (the solvent was DCM). And for TCPP, standard solutions with six different concentrations (1, 2, 5, 10, 20 and 40 µg/mL) were obtained by diluting TCPP liquids (the solvent was DCM). 1 µL of each standard solution was injected into the GC injector to establish a six-point calibration line. The peak area of GC-MS was found to be linearly related to the amount in the standard solutions (the product of the standard concentration and the injection volume of 1 µL). The slope of the linear relationship was obtained by fitting eq. (1) of the main text to the data points (six pairs of peak area and injection amount). The results were assumed valid when the R^2 value of the fitted line was greater than 0.99. In this way, the value of the liquid-based calibration constant (i.e., k_l in eq. (1) of the main text) was obtained. In our experiments, the value of k_l was updated twice or thrice a week to correct the status changes of the GC-MS.

The limit quantitation (LOQ) was set to be 0.6 ng and 1 ng for DiBP and TCPP, respectively. Below these levels, the linear relationship was no longer valid. In addition, the injection amount should not exceed 30 ng and 40 ng for DiBP and TCPP, respectively, because the relationship might also not be linear above these levels.

3. The calibration of GC-MS for sorbent tubes

To eliminate the effect of the status changes of the GC-MS on the accuracy of the results, the calibration of GC-MS for sorbent tubes was established by the internal standard method. The standard solutions of both DiBP and TCPP in DCM (100, 200, 300, 400, 500, 600, and 800 ng, 10 µL solutions with concentrations of 10–80 µg/mL) were injected into the sorbent tubes to establish a seven-point calibration line. Meanwhile, 2 µL solution of BB (100 µg/mL, 200 ng in total) in DCM was injected into each sorbent tube as internal standards. The sorbent tubes were analyzed using the procedures described above. The ratio of the analyte peak area to the BB peak area was linearly related to the ratio of the analyte amount to the BB amount. The slope of the linear relationship was used to determine the analyte amount collected in sorbent tubes. The calibration line was considered to be valid when the R^2 of the calibration line was larger than 0.99.

4. Chemicals used in the experiments

High purity liquids of DnBP (purity > 99%, 152641-100ML) and BB (purity > 98%, B9550-250ML) were purchased from Sigma-Aldrich Co., LLC. TCPP liquid (purity > 98%, T829900-500g), benzyl butyl phthalate (purity > BBzP, 98%, 36927-250MG), and DCM (purity > 99.9%, D807825-4) were purchased from Mackin Inc. (Shanghai, China).

Section S4. Temperature dependence of the gaseous concentrations of DiBP and TCPP measured by sorbent tubes

The temperature dependence of saturated gas-phase concentrations of pure chemicals is always described by the Clausius–Clapeyron equation [6]. Over a narrow temperature range (e.g., from 0 °C to 30 °C), the Clausius–Clapeyron equation is,

$$\ln C_{sat} = -\frac{\Delta H_{vap}}{RT} + B \quad (S1)$$

where B is a constant for a given chemical; T is the temperature, K; ΔH_{vap} is the enthalpy of vaporization for pure chemical liquids, which can be treated as constant over a narrow temperature range (e.g., 0 °C to 30 °C) [6]; R is the universal gas constant, 8.314 J/(mol K); and C_{sat} is the saturated gas-phase concentration of pure chemical, i.e., the gaseous concentration at the outlet of the source chamber (presented as C_g in the figure).

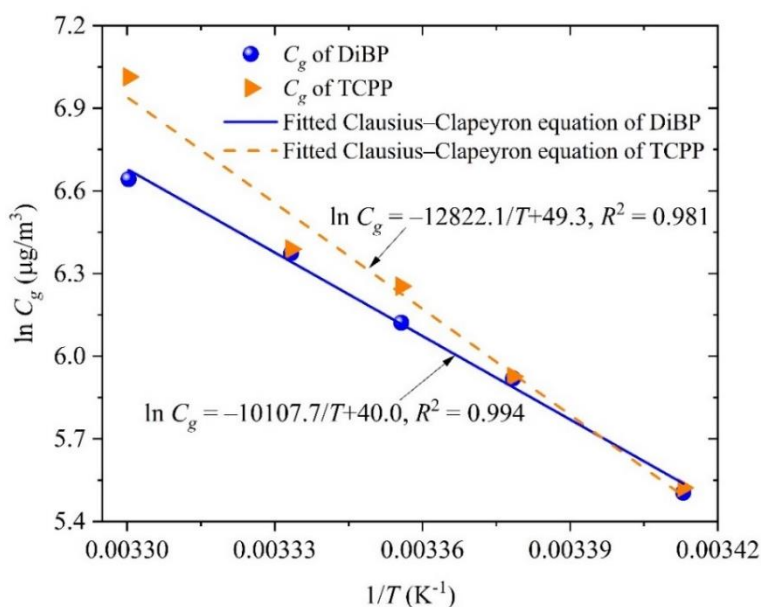


Figure S4. Comparison of the Clausius–Clapeyron equation with gaseous concentrations of DiBP and TCPP measured by the sorbent tubes (packed with Tenax TA) at different temperatures (20 °C, 23 °C, 25 °C, 27 °C, and 30 °C). Points represent the measured results, the line with color similar to the points represents the fitted line of these points by using Clausius–Clapeyron equation.

The Clausius–Clapeyron equation was used to fit C_g of DiBP and TCPP at different temperatures. The comparison of the fitted line with the measurements is provided in Figure S4, which indicates high fitting precision ($R^2 > 0.98$). The slope of the fitted line equals $\Delta H_{vap}/R$. According to the fitted slope, ΔH_{vap} of DiBP was found to be 84.0 kJ/mol, which was consistent with the value reported by Wu et al. [7] (92 ± 10 kJ/mol); and ΔH_{vap} of TCPP was found to be 107 kJ/mol, which also agreed well with the value reported in the literature (101 kJ/mol [8]). The above consistence supports the reliability of C_g measured by the sorbent tubes.

Section S5. Time variation of the SPME calibration constant (β) of DiBP and TCP

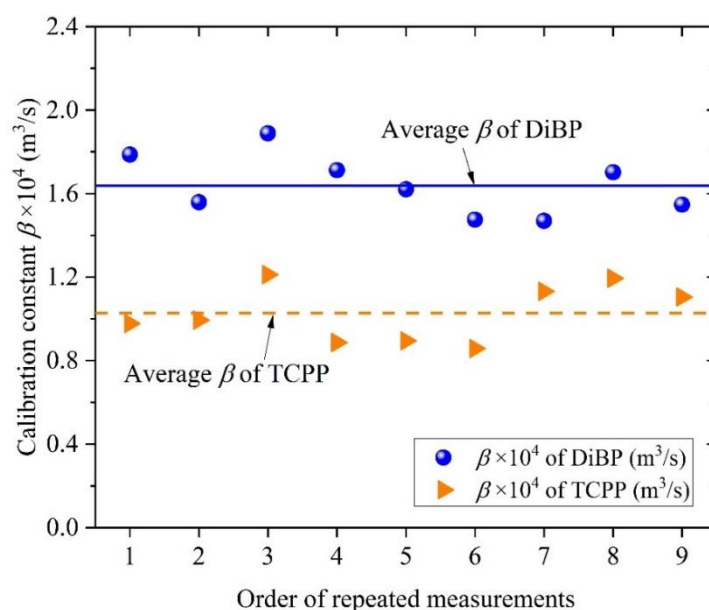


Figure S5. Time variation of the SPME calibration constant (β) of DiBP and TCP. Nine similar measurements were repeated in three months. The blue solid line represents the average β of DiBP ($1.64 \times 10^{-4} \text{ m}^3/\text{s}$), and the orange dash line represents the average β of TCP ($1.03 \times 10^{-4} \text{ m}^3/\text{s}$).

The measurements were conducted in the experimental system similar to that introduced in Section S2 (i.e., the pre-experiments to obtain the sorption process of SPME). SPMEs were inserted into the outlet of the source chamber for different lengths of time (similar to the time series in Table S2). The measurements were all conducted at 25°C , with a flow rate of $75 \text{ mL}/\text{min}$. The values of β were obtained by the procedures similar to those in “experiment 1” of the main text. The measurements were separately conducted on different dates of last three months of 2020. Specifically, β 's of DiBP were measured on Oct. 13, Oct. 15, Oct. 19, Nov. 27, Nov. 29, Dec. 1, Dec. 15, Dec. 16, and Dec. 17 (corresponding to order 1–9 for DiBP in Figure S5); and β 's of TCP were measured on Oct. 22, Oct. 30, Nov. 4, Dec. 6, Dec. 7, Dec. 8, Dec. 11, Dec. 13, and Dec. 14 (corresponding to order 1–9 for TCP in Figure S5).

As shown, the values of β were relatively stable over the three-month period. For DiBP, the relative standard deviation of these nine measurements was 8.7%, and the maximum relative deviation between a single β and the average β was less than 15%. For TCP, the relative standard deviation of these nine measurements was 13%, and the maximum relative deviation between a single β and the average β was less than 18%. Overall, the stability for TCP was relatively lower, yet still acceptable. The deviations of β among repeated measurements might be due to the experimental errors.

It should be noted that the β values obtained here were significantly different to those obtained in “experiment 1” of the main text, i.e., $1.64 \times 10^{-4} \text{ m}^3/\text{s}$ (here) versus $2.92 \times 10^{-4} \text{ m}^3/\text{s}$ (main text) for DiBP and $1.02 \times 10^{-4} \text{ m}^3/\text{s}$ (here) versus $8.74 \times 10^{-5} \text{ m}^3/\text{s}$ (main text) for TCP. The difference may be caused by two reasons. First, the experimental setup was a little different between them. The sampling tube of the SPME-based active sampler was eliminated in the measurements here, i.e., SPME was directly inserted into the source chamber coated with SVOC liquids. The difference between the diameter of the source chamber and that of the sampling tube of the SPME sampler (17.2 mm vs. 4 mm) leads to different air velocities over the SPME coating, subsequently leads to different convective mass-transfer coefficients over the coating surface (h_m , which is a function of air velocity), and finally leads to different β ($\beta = k \times h_m$). Second, the GC-MS was turned off for several

days at the end of 2020 (due to the new-year vacation) and restarted at the beginning of 2021. The experiments in the main text were all conducted after the restart. Before the restart, several accessories of the GC-MS were replaced, including the septum and the liner of the GC-MS injector. The restart and replacement of the GC-MS accessories may cause changes to the ratio of the transfer efficiency of the liquid samples to that of the SPME samples in GC-MS (i.e., k in main text), and subsequently result in different β .

Section S6. Experiments for benzyl butyl phthalate (BBzP)

Another experiment (experiment 3) was conducted to preliminarily evaluate the applicability of the SPME-based active sampler for low volatile SVOCs. BBzP was chosen as the target SVOC. The experimental system and procedures were almost similar to those in “experiment 1” and “experiment 2” of the main text, except for three differences. First, the one-hour tube sorption was not required in “experiment 3”, i.e., SPME was inserted into the sampling tube immediately after connecting a fresh SPME sampler to the source chamber. Second, the sampling time of SPME was kept constant instead of a series of different times. Third, the sampling times of SPME and sorbent tubes were set to be 2 hours and 4 hours, respectively, because C_g of BBzP was two orders of magnitude lower than those of DiBP and TCPP (longer time is therefore required to collect sufficient amount of BBzP). The chemical analysis of BBzP was similar to that of DiBP. The calibration constant of SPME (β) was obtained by dividing the “equivalent” sorption amount by the sampling time and the corresponding C_g measured by the sorbent tubes. In this way, β involves the effects of the sampling-tube loss of gaseous BBzP. Results of “experiment 3” were given in Table S3 (the values of β), Table S4 (comparison of C_g measured by SPME with C_g measured by sorbent tubes), and Figure S6 (temperature dependence of C_g measured by sorbent tubes). Compared to TCPP and DiBP, similar results were obtained for BBzP, except that the stability of C_g measured by SPME was lower than that of sorbent tubes.

Table S3. SPME calibration constants (β) of BBzP measured at different temperatures.

SVOCs	Temperature (°C)	$\beta_T \times 10^4$ (m ³ /s) ^a	$\beta \times 10^4$ (m ³ /s) ^b	RSD (%) ^c
BBzP	20	0.598	0.718	15
	25	0.798		
	30	0.758		

^a β_T is the calibration constant of SPME measured at a certain temperature.

^b β is the average of the calibration constant of SPME measured at three temperatures.

^c RSD is the relative standard deviation of β measured at three temperatures.

Table S4. Comparison of the gaseous concentrations (C_g) of BBzP measured by the sorbent tubes (packed with Tenax TA) with those measured by the SPME-based active sampler.

Temperature (°C)	Results of Tenax TA		Results of SPME		RD (%) ^c
	C_g (µg/m ³) ^a	RSD (%) ^b	C_g (µg/m ³) ^a	RSD (%) ^b	
20	3.08	8.3	— ^d	—	—
23	4.62	18	4.07	15	12
25	5.48	13	— ^d	—	—
27	8.09	8.8	8.16	30	0.87
30	11.5	7.1	— ^d	—	—

^a C_g is the average gaseous concentration of multiple measurements (6–10 times). ^b RSD is the relative standard deviation of C_g obtained by multiple measurements. ^c RD is the relative deviation between C_g measured by Tenax TA sorbent tubes and C_g measured by SPME ($|C_{g_Tenax} - C_{g_SPME}| / C_{g_Tenax} \times 100\%$). ^d C_g not measured by SPME method because corresponding experiments were only conducted at 23 °C and 27 °C.

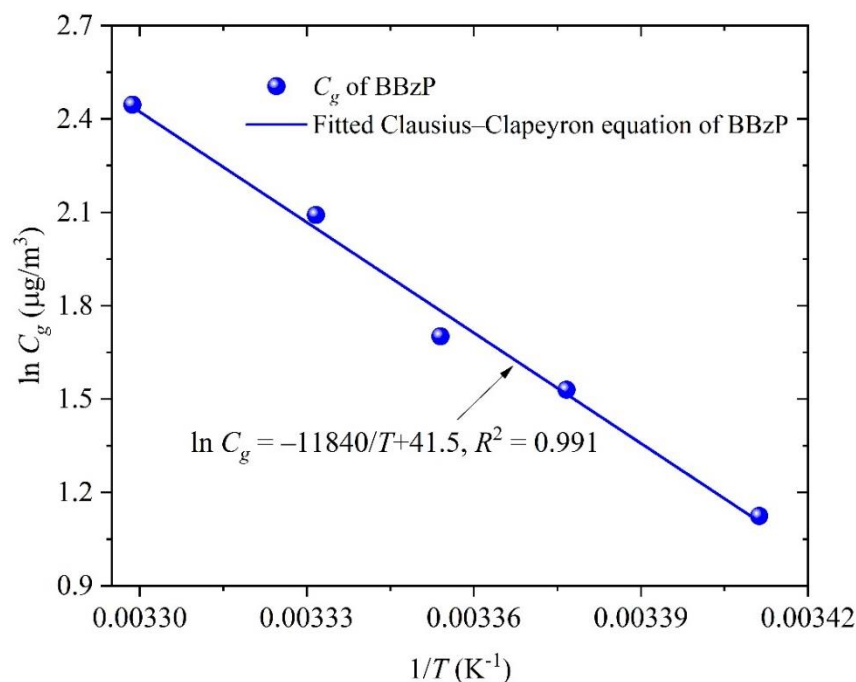


Figure S6. Comparison of the Clausius–Clapeyron equation with gaseous BBzP concentrations measured by the sorbent tubes (packed with Tenax TA) at different temperatures (20 °C, 23 °C, 25 °C, 27 °C, and 30 °C).

References

1. Cao, J.; Xiong, J.; Wang, L.; Xu, Y.; Zhang, Y. Transient method for determining indoor chemical concentrations based on SPME: Model development and calibration. *Environ. Sci. Technol.* **2016**, *50*, 9452–9459, DOI: 10.1021/acs.est.6b01328.
2. Cao, J.; Weschler, C.J.; Luo, J.; Zhang, Y. C_m-history method, a novel approach to simultaneously measure source and sink parameters important for estimating indoor exposures to phthalates. *Environ. Sci. Technol.* **2016**, *50*, 825–834, DOI: 10.1021/acs.est.5b04404.
3. Ouyang, G.; Pawliszyn, J. A critical review in calibration methods for solid-phase microextraction. *Anal. Chim. Acta* **2008**, *627*, 184–197, DOI: 10.1016/j.aca.2008.08.015.
4. Ai, J. Solid phase microextraction for quantitative analysis in nonequilibrium situations. *Anal. Chem.* **1997**, *69*, 1230–1236, DOI: 10.1021/ac9609541.
5. Ai, J. Headspace solid phase microextraction. Dynamics and quantitative analysis before reaching a partition equilibrium. *Anal. Chem.* **1997**, *69*, 3260–3266, DOI: 10.1021/ac970024x.
6. Schwarzenbach, R.P.; Gschwend, P.M.; Imboden, D.M. *Environmental Organic Chemistry*; John Wiley & Sons: New York, US, 2005.
7. Wu, Y.; Eichler, C.M.; Chen, S.; Little, J.C. Simple method to measure the vapor pressure of phthalates and their alternatives. *Environ. Sci. Technol.* **2016**, *50*, 10082–10088, DOI: 10.1021/acs.est.6b02643.
8. Wang, Q.; Zhao, H.; Wang, Y.; Xie, Q.; Chen, J.; Quan, X. Determination and prediction for vapor pressures of organophosphate flame retardants by gas chromatography (in Chinese). *Chinese Journal of Chromatography* **2017**, *35*, 1008–1013, DOI: CNKI:SUN:SPZZ.0.2017-09-015.